Organic Electronics 83 (2020) 105772

Contents lists available at ScienceDirect

Organic Electronics

journal homepage: http://www.elsevier.com/locate/orgel

Increased stripe density of slot-coated PEDOT:PSS using a meniscus guide with linearly tapered μ-tips for OLEDs

Jinyoung Lee, Jongwoon Park *

School of Electrical, Electronics & Communication Engineering, Korea University of Technology and Education, Cheonan, 330-708, South Korea

ARTICLE INFO

Keywords:
Slot-die head
Meniscus guide
Linearly tapered μ-tip
Stripe coating
OLEDs

ABSTRACT

We have performed slit coatings using a slot-die head with μ-tips in various shapes (rectangular-shaped, partially tapered, and linearly tapered μ-tips) to achieve high-density fine organic stripes for potential applications in solution-processable organic light-emitting diode (OLED) displays. The fluid dynamics of an aqueous poly(3,4-ethylenedioxythiophene):poly(4-styrenesulfonate) (PEDOT:PSS) in the presence of those μ-tips has been analyzed based on the electronic–hydraulic analogy. It is demonstrated that both line breakup occurring at low coating speeds with the rectangular-shaped narrow μ-tip and line broadening appearing with the rectangular-shaped wide μ-tip are avoidable using the linearly tapered μ-tip. It is attributed that the hydraulic resistance inside the slot-die head is decreased and the meniscus is well controlled by the linearly tapered structure. It also has a big advantage in the fabrication of multiple PEDOT:PSS stripes that the spacing between stripes can be kept constant. To fabricate high-density fine PEDOT:PSS stripes, we have devised a slot-die head with two meniscus guides embedded, each of which has 175 linearly tapered μ-tips. Using such a slot-die head, we have successfully fabricated 350 PEDOT:PSS stripes and 300 OLED stripes (59 stripes per inch) with the luminance of 350 cd/m^2 at 5 V.

1. Introduction

Fine stripe patterns are demanded for various applications including solution-processable organic light-emitting diode (OLED) flat panel displays [1], large-area OLED lighting panels with metal shunting lines [2,3], touch screen panels with metal mesh [4], solution-processed micro-stripe antennas [5], sensors [6], etc. Especially for OLED display applications, highly uniform organic stripes as narrow as a pixel width (<100 μm) and as dense as a pixel array are required. The formation of solution-processable organic stripes provides an approach to remove the pixel bank structure used to confine ink droplets [7–9]. To this end, printing processes (e.g., inkjet, nozzle, gravure, offset, etc.) rather than coating processes (e.g., slot, blade, spin, spray, etc.) are preferred because of their capability of high-resolution lateral patterning [10–17]. However, coating methods have a big advantage over printing methods that the maintenance of equipment is facile and the choice of solutions is flexible. As such, slot-die coating was also employed to fabricate millimeter-wide stripe patterns for organic photovoltaics using a meniscus guide embedded into a slot-die head together with a shim [11]. Through the numerical simulations of a slot-die head for multiple stripes, it was shown that the homogeneous flow dynamics was affected by T-die and a proper shim structure [18,19]. Recently, we demonstrated that micrometer-wide stripe coating of an aqueous poly(3,4-ethylenedioxythiophene):poly(4-styrenesulfonate) (PEDOT:PSS) was feasible using the slot-die head with multiple μ-tips [20]. The μ-tips fabricated by a laser cutter were protruded from the head lip in such a way that the meniscus was formed between the μ-tip and the substrate, rendering the coated stripe well defined. We fabricated 150 stripes (25.4 stripes per inch (SPI)) using 150-μm-wide rectangular-shaped μ-tips. However, the stripe density is still too low for applications in large-area OLED displays.

To increase it further, one has to reduce the μ-tip width and increase the number of μ-tips because the stripe width is proportional to the μ-tip width and the stripe density is boosted with increasing number of μ-tips. In this case, however, two troublesome issues arise; 1) The electronic–hydraulic analogy (i.e., just as all wires have some resistance to current, the μ-tip has some resistance to fluid flow) would appear. The resistance to fluid flow may increase as the μ-tip becomes narrow, causing multiple stripe coating unstable. To tackle it, therefore, a μ-tip with a new configuration is required. 2) Stripe merging may appear

* Corresponding author.
E-mail address: pjwup@koreatech.ac.kr (J. Park).

https://doi.org/10.1016/j.orgel.2020.105772
Received 21 January 2020; Received in revised form 23 March 2020; Accepted 9 April 2020
Available online 19 April 2020

during high-density stripe coating. If μ-tips are deployed closely, a low-viscosity solution is spread along the head lip due to lateral capillary force and thus the fluids from the neighboring outlets are easily merged. To raise the stripe density, therefore, a slot-die head with a new configuration is also demanded. With an attempt to tackle those issues, we have first made a comparative investigation on the coating behaviors of a slot-die head with μ-tips in various shapes (rectangular-shaped, partially tapered, or linearly tapered μ-tips). It is demonstrated that the linearly tapered μ-tip offers a way of increasing the maximum coating speed without line breakup, rendering the stripe narrower and thinner. To obtain high-density fine organic stripes, we come up with the slot-die head with two meniscus guides embedded where linearly tapered μ-tips are formed and deployed without overlapping. Using such a slot-die head, we have successfully fabricated 350 PEDOT:PSS stripes and 300 OLED stripes (59 SPI) with the luminance of 350 cd/m^2 at 5 V.

2. Experiment

We performed slot coatings of multiple stripes as well as a single stripe using a roll-to-roll (R2R) slot coater that consists of a slot head module, vacuum dry unit (5×10^{-4} Torr), tension and motion controller for the web (web speed: 0.1 mm/s ~ 100 mm/s), syringe pump system (11 Elite I/W Single, Harvard Apparatus, 0.18 μl/min ~159.8 ml/min), O_3 plasma treatment (0.3 kW), and ionizers. Shown in Fig. 1 is the slot-die head (head size: 200 mm × 40 mm × 58 mm, cavity (ink distribution chamber): 156 mm × 2 mm) used for experiments. In the conventional slot-die head for multiple stripe coating [20], there is only a single pair of upstream and downstream lips, between which the dual plate (a shim with slit channels (waterways) and a meniscus guide with μ-tips) is inserted. In this case, the slot-die head is divided into two parts; the upstream (front) die and downstream (rear) die. In the slot-die head we used for high-density stripe coating, however, there exist two pairs of upstream and downstream lips. In this case, the slot-die head is divided into three parts; the upstream (front) die, down/upstream (middle) die, and downstream (rear) die. For coating of a single stripe (1 line), one dual plate with a single μ-tip was embedded in the head. For coating of multiple stripes (175 lines), one dual plate with multiple μ-tips was embedded. For coating of high-density stripes (350 lines), two dual plates with multiple μ-tips were embedded in the head (one between the front and middle dies and the other between the middle and rear dies). When two dual plates are embedded, the μ-tips are arranged in such a way that the number of coated stripes within the effective coating width (=150 mm) is doubled without overlapping. Namely, a μ-tip in one meniscus guide is centered between two μ-tips in the other meniscus guide (Fig. 1(b)).

A meniscus guide with μ-tips and a shim were fabricated by a laser cutter using a polyimide (PI) film with high heat resistance. Shown in Fig. 2 are the optical images of a meniscus guide and a shim superimposed. We fabricated four different shapes of μ-tips with the length of 250 μm; a rectangular-shaped narrow (50-μm-wide) μ-tip (hereinafter referred to as RN-TIP, Fig. 2(a)), a rectangular-shaped wide (120-μm-wide) μ-tip (RW-TIP, Fig. 2(b)), a partially tapered μ-tip (PT-TIP, Fig. 2(c)), and a linearly tapered μ-tip (LT-TIP, Fig. 2(d)). In the tapered μ-tips, the μ-tip width was reduced from 120 μm to 50 μm. The minimum μ-tip width was determined to be 50 μm because the μ-tip became ill defined if it was machined to a width below 50 μm. The coating gap was fixed to be 20 μm. We used the meniscus guide as thick as 175 μm to ensure the firmness of μ-tip and the shim plate as thin as 50 μm. A solution flows out of the slit channel (waterway or outlet, Fig. 2 (c)), the width of which is the same as the μ-tip width. The cross-sectional area of each channel is equal to be slit channel width × shim thickness. The aqueous PEDOT:PSS (Clevios AI 4083) solution was coated on a 170-mm-wide polyethylene terephthalate (PET) film roll (the effective coating width was 150 mm). As a wetting agent, we added a 0.2 wt% fluorosurfactant into the pristine PEDOT:PSS solution. The fluid distribution near the μ-tip was measured by an area scan camera (acA1300-30 gm, BASLER). The coated PEDOT:PSS films were pre-dried in a vacuum dry unit for 10 min and hard-baked on a hot plate at 80 °C for 20 min. The profiles (width and thickness) of coated stripes were measured by 3D optical surface profiler (NV 6300, ZYGO).

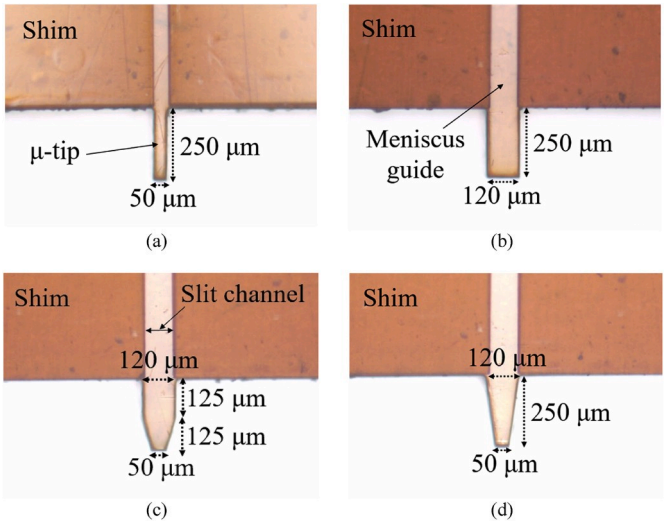

Fig. 2. Optical images of a shim and a meniscus guide superimposed; (a) rectangular-shaped narrow (50-μm-wide) μ-tip (RN-TIP), (b) rectangular-shaped wide (120-μm-wide) μ-tip (RW-TIP), (c) partially tapered μ-tip (PT-TIP), and (d) linearly tapered μ-tip (LT-TIP) fabricated by a laser cutter using heat-resistant PI film.

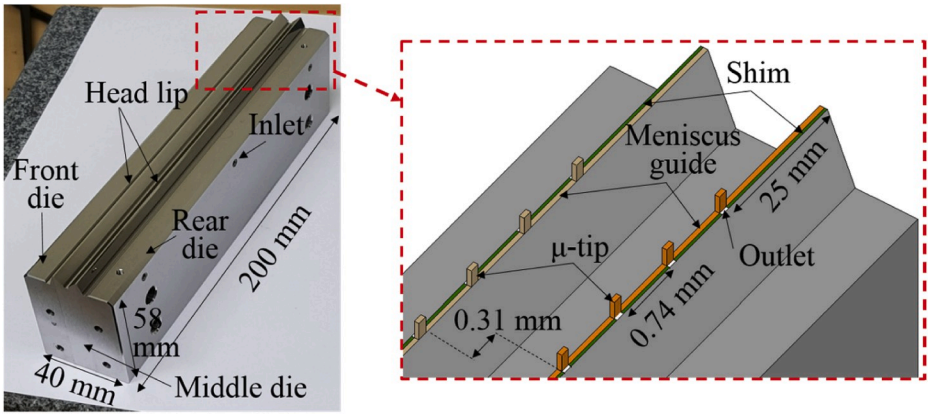

Fig. 1. Slot-die head (200 mm × 40 mm × 58 mm) with two pairs of upstream and downstream lips.

3. Results and discussion

We have first coated a single PEDOT:PSS stripe to investigate the effect of the μ-tip configuration on the fluid dynamics and thin-film property. Presented in Fig. 3 are the optical images and profiles of a single PEDOT:PSS stripe coated a maximum coating speed and summarized in Table 1 is the measured width and thickness values for different coating speeds. For single stripe coating, the flow rate was 0.8 μl/min. We can achieve a narrow and thin stripe at a maximum coating speed, above which line breakup occurs or the stripe width becomes smaller than the μ-tip width (i.e., coating defects appear). It is obvious from Table 1 that the stripe width and thickness increase with decreasing coating speed (below the maximum coating speed). The maximum coating speed with RN-TIP is as low as 13 mm/s, whereas it is increased to 17 mm/s with RW-TIP and up to 20 mm/s using PT- and LT-TIPs. Since the meniscus is formed between the μ-tip and the substrate, the stripe width is proportional to the μ-tip width. As such, RW-TIP provides the widest (124-μm-wide) stripe. Using LT-TIP, however, we have achieved the stripe pattern as narrow as that (98~99 μm) obtained by RN-TIP at a higher coating speed. This behavior can be explained based on the electronic–hydraulic analogy. Fig. 4 shows the equivalent circuit of the slot-die head with μ-tips. A solution (ink) corresponds to the electrical current in the circuit. The inlet where the PEDOT:PSS solution is supplied corresponds to the electrode contact and hence the flow rate corresponds to a voltage source (V_s). R_S represents the resistance to fluid flow (hydraulic resistance) through the slit channel (waterway) inside the slot-die head, which can be evaluated by Poiseuille's law for resistance through a tube [21–23]. The hydraulic resistance is written as

$$R_S = \frac{8\eta l}{\pi r^4} \tag{1}$$

where η denotes the viscosity of a fluid, r the radius of a tube, and l its length. From Eq. (1), it is apparent that increasing the cross-sectional area (= slit channel width × shim thickness) of each slit channel results in a decrease in the R_S value. R_L indicates the resistance to fluid flow in the head lip. Since the head lip is hydrophilic (its contact angle is about 16°), the R_L value would be relatively very low. R_T represents the resistance to fluid flow in a μ-tip. The R_T value can be estimated by

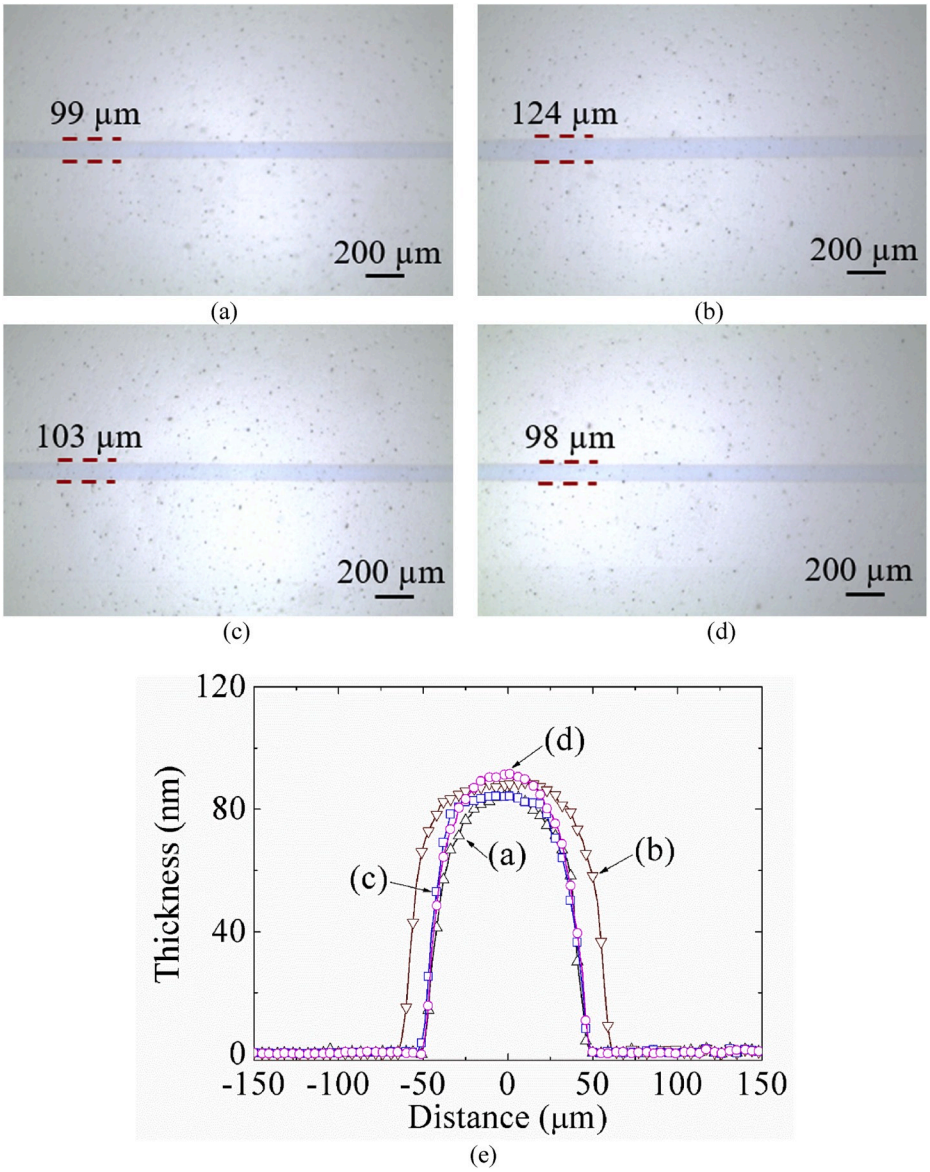

Fig. 3. Optical images of a single PEDOT:PSS stripe coated with (a) RN-TIP at the maximum coating speed of 13 mm/s, (b) RW-TIP at 17 mm/s, (c) PT-TIP at 20 mm/s, and (d) LT-TIP at 20 mm/s and (e) measured profiles of those stripes.

Table 1
Measured width (W) and thickness (T) of a single PEDOT:PSS stripe for different coating speeds (V).

RN-TIP			RW-TIP			PT-TIP			LT-TIP		
V (mm/s)	W (μm)	T (nm)	V (mm/s)	W (μm)	T (nm)	V (mm/s)	W (μm)	T (nm)	V (mm/s)	W (μm)	T (nm)
8	151 ± 3	106 ± 2	10	212 ± 2	97 ± 2	10	165 ± 3	126 ± 4	10	154 ± 1	139 ± 4
10	133 ± 2	98 ± 3	14	143 ± 3	91 ± 3	14	127 ± 2	106 ± 2	14	118 ± 2	115 ± 3
13	99 ± 1	85 ± 3	17	124 ± 2	87 ± 2	17	114 ± 3	98 ± 3	17	109 ± 2	108 ± 3
–	–	–	–	–	–	20	103 ± 2	83 ± 2	20	98 ± 2	89 ± 2

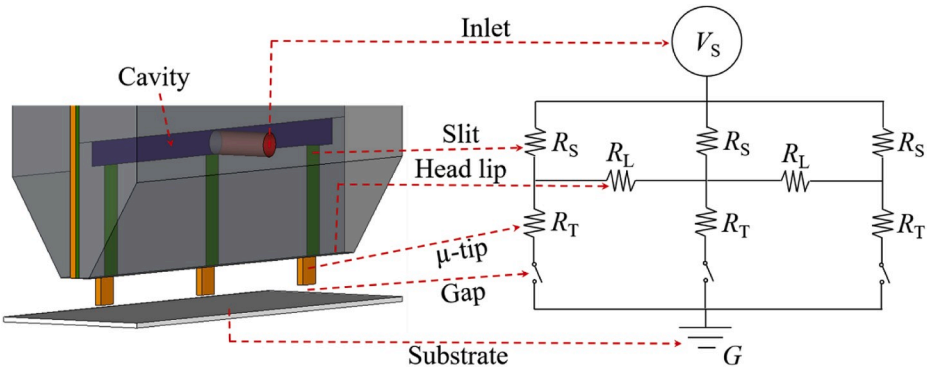

Fig. 4. Equivalent circuit of a slot-die head with the dual plate embedded.

$$R_T = \frac{\rho L}{A} \quad (2)$$

where ρ is the resistivity, L the μ-tip length, and A the cross-sectional area of μ-tip. Since the PEDOT:PSS solution flows along the outer surface of the μ-tip, A is determined mainly by the μ-tip width (i.e., μ-tip configuration). The switch in Fig. 4 represents the coating gap. If the solution bridges the gap difference between the μ-tip and the substrate (i.e., the solution reaches the substrate), the switch is on. In the beginning, the fluid from the slit channel is distributed along the head lip due to strong lateral capillary flow (low R_L) and off switch mode (high resistance). Once the switch is on, all the solution (current) flows through the μ-tip (R_T). Even so, some fluid is still distributed along the head lip because of the resistance to flow in the μ-tip.

From Fig. 2, RN-TIP is expected to show the highest R_S and R_T values.

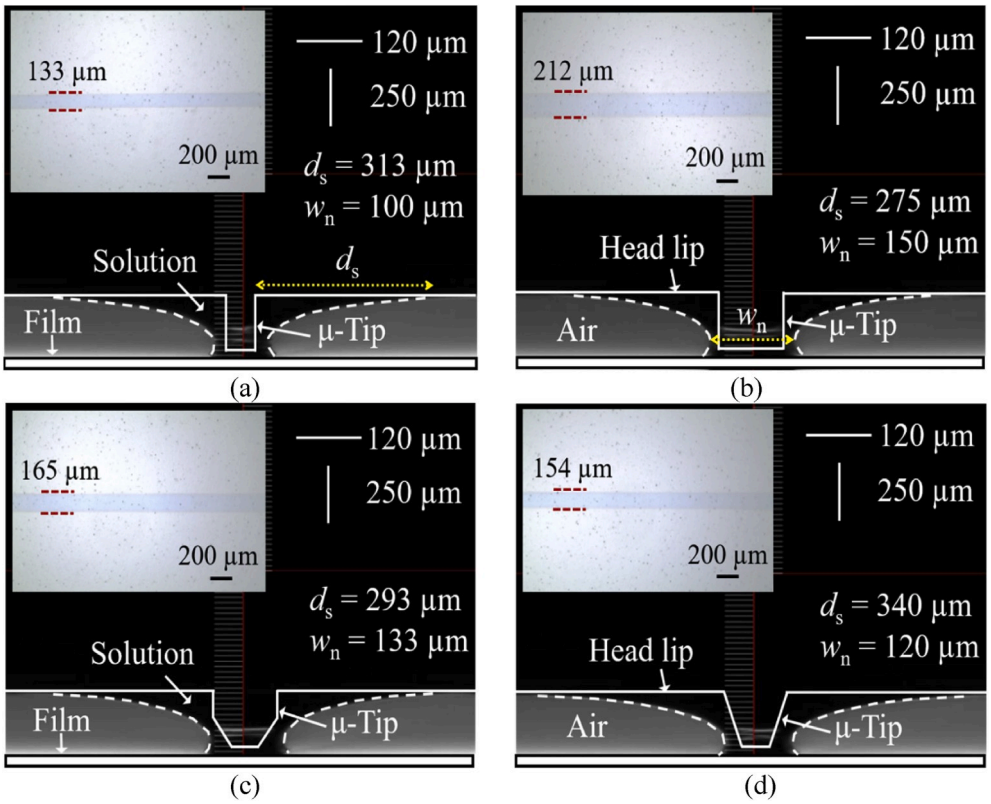

Fig. 5. Measured fluid distribution during stripe coating at 10 mm/s using the (a) RN-TIP, (b) RW-TIP, (c) PT-TIP, and (d) LT-TIP.

R_S is the highest because the slit channel is the narrowest (i.e., the radius of a tube in Eq. (1) is reduced), possibly causing a reduction of the current (fluid) flowing through R_T (μ-tip) to the ground (substrate). In addition, R_T is the highest with RN-TIP because A in Eq. (2) is the lowest, bringing in line breakup even at low coating speeds (above 13 mm/s). Of those μ-tips, RW-TIP is expected to show the lowest R_S and R_T values because the slit channel is the widest and A is the largest, thereby increasing the maximum coating speed to 17 mm/s. However, RW-TIP provides the widest (124-μm-wide) stripe because the stripe width is in proportion to the μ-tip width. From this, we can deduce that the upper end of the μ-tip is desirable to be wide and its lower end should be narrow. The tapered μ-tip is such a case in point. The effect of R_T (μ-tip configuration) on the fluid dynamics can be clearly seen in Fig. 5 showing the measured fluid distribution near the μ-tip at the fixed coating speed of 10 mm/s (the flow rate is also fixed) and in Fig. 6 at the maximum coating speed. To quantify its effect, we have measured the distance (d_s) the PEDOT:PSS solution spreads laterally along the head lip from the μ-tip (Fig. 5(a)) and the narrowest width (w_n) of the fluid stream near the μ-tip end (Fig. 5(b)). At the coating speed of 10 mm/s, the measured d_s value using RN-, RW-, PT-, and LT-TIPs is about 313 μm, 275 μm, 293 μm, and 340 μm, respectively. It is noted that the amount of fluid flowing out of the slit channel is reduced with decreasing cross-sectional area of the channel (i.e., increasing R_S), which is described by Hagen–Poiseuille's law [21];

$$Q = \frac{\Delta p}{R_s} \tag{3}$$

where Q is the volumetric flow rate and Δp is the pressure difference. As such, a direct comparison of RN-TIP with the others in terms of the fluid distribution at a fixed (the same) flow rate is not fair. Namely, a fair comparison can be made when the slit channel width is the same. It is observed from Fig. 5 (b)–(d) that the d_s value increases with decreasing A (μ-tip width). Less fluid is distributed along the head lip with RW-TIP due to low R_T, whereas more fluid is distributed along the head lip with LT-TIP due to high R_T, which is in accordance with the electronic–hydraulic analogy. At the maximum coating speed, the measured d_s value using RN-, RW-, PT-, and LT-TIPs is about 276 μm, 260 μm, 223 μm, and 196 μm, respectively (Fig. 6). From Figs. 5 and 6, it is apparent that the d_s value is reduced with increasing coating speed. At the maximum coating speed, the d_s value is rather decreased with decreasing A (μ-tip width). One may expect that the maximum coating speed would be the highest with RW-TIP because both R_S and R_T are the lowest. In fact, the line does not break at speeds above the maximum coating speed (17 mm/s). As evident in Fig. 6(b), however, the w_n value (=126 μm) is almost the same as the tip width (=120 μm) at 17 mm/s and hence the PEDOT:PSS solution appears inwards from both edges of the tip end (i.e., w_n becomes smaller than the μ-tip width) above 17 mm/s, causing a tiny wobble in the meniscus and thus unstable stripe coatings (i.e., line is not straight). It would also have a negative effect in multiple stripe coating, which will be discussed later with experiment results. Such a phenomenon does not appear with RN-, PT-, and LT-TIPs. Instead, line breakup occurs when the coating speed is greater than the maximum coating speed. Due to low R_S, more fluid flows out of the slit channel in the presence of LT-TIP. Due to high R_T, however, a large amount of fluid is distributed along the head lip (the d_s value is highest) at 10 mm/s. At the same time, w_n (=120 μm) is much larger than the width of μ-tip end (50 μm). Such a large amount of fluid existing along the head lip and near the μ-tip end contributes to an increase in the coating speed and in turn the w_n value can be the lowest due to the linearly tapered configuration at the maximum coating speed without line breakup, rendering d_s (=196 μm) and w_n (=85 μm) the lowest (Fig. 6 (d)). That is why the d_s value is rather decreased with decreasing A (μ-tip width) at the maximum coating speed. At 20 mm/s, the w_n value (=103 μm) with PT-TIP is larger than that (=85 μm) with LT-TIP. Therefore, it is desirable to use the linearly tapered μ-tip for the fabrication of a fine

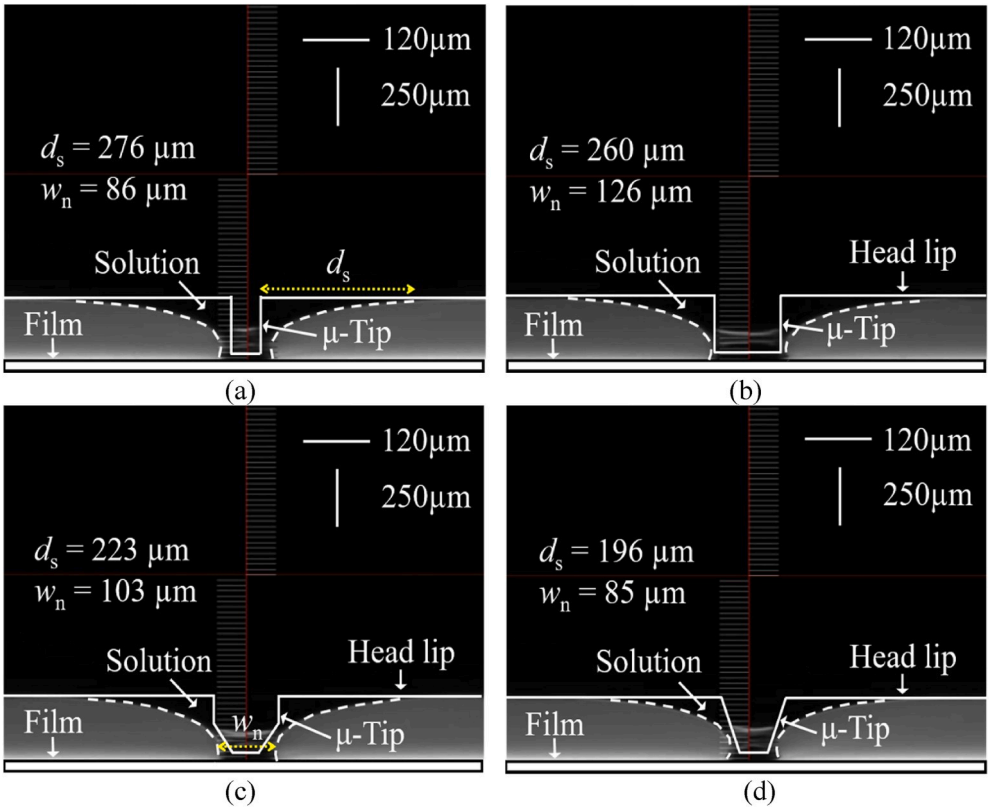

Fig. 6. Measured fluid distribution during stripe using the (a) RN-TIP at the maximum coating speed of 13 mm/s, (b) RW-TIP at 17 mm/s, (c) PT-TIP at 20 mm/s, and (d) LT-TIP at 20 mm/s.

stripe.

Before coating multiple stripes, we have investigated the effect of single stripe coating on the emission property of OLEDs. To this end, we have coated the PEDOT:PSS stripe on a 150-nm-thick indium-tin-oxide (ITO) pre-coated on a glass substrate using the slot-die head with LT-TIP (Fig. 7(a)). Using a thermal evaporator, we have then fabricated a phosphorescent green OLED with the emission area as large as 2 mm × 2 mm. Outside the emission area, a 1.5-μm-thick photoresistor (PR) was coated as an insulation area (Fig. 7(a)). As depicted in Fig. 7(b), the OLED device consists of 40-nm-thick N,N′-Bis(3-methylphenyl)-N,N′-diphenylbenzidine (TPD) for a hole transport layer (HTL), 15-nm-thick 4,4′-bis(N-carbazolyl)-1,1′-biphenyl (CBP) for an emission layer (EML), 10-nm-thick 4,7-diphenyl-1,10-phenanthroline (Bphen) for a hole/exciton blocking layer (HBL), 30-nm-thick Tris(8-hydroxyquinoline)aluminum (Alq_3) for an electron transport layer (ETL), 1-nm-thick lithium fluoride (LiF) for an electron injection layer (EIL), and 100-nm-thick aluminum (Al). In the emitting layer, Tris[2-(p-tolyl)pyridine-C2,N)]iridium(III) ($Ir(mppy)_3$) was doped (8 wt%) for green emission. For comparison, we also fabricated OLED without the PEDOT:PSS stripe. As evident in Fig. 7(c)–(d), the strong light-emitting stripe is observed from OLED with the PEDOT:PSS stripe. Strong light emission is observed because the PEDOT:PSS stripe acts as a hole injection layer (HIL) and thus a large amount of current flows through the narrow stripe. As a result, leakage current also increases, causing a

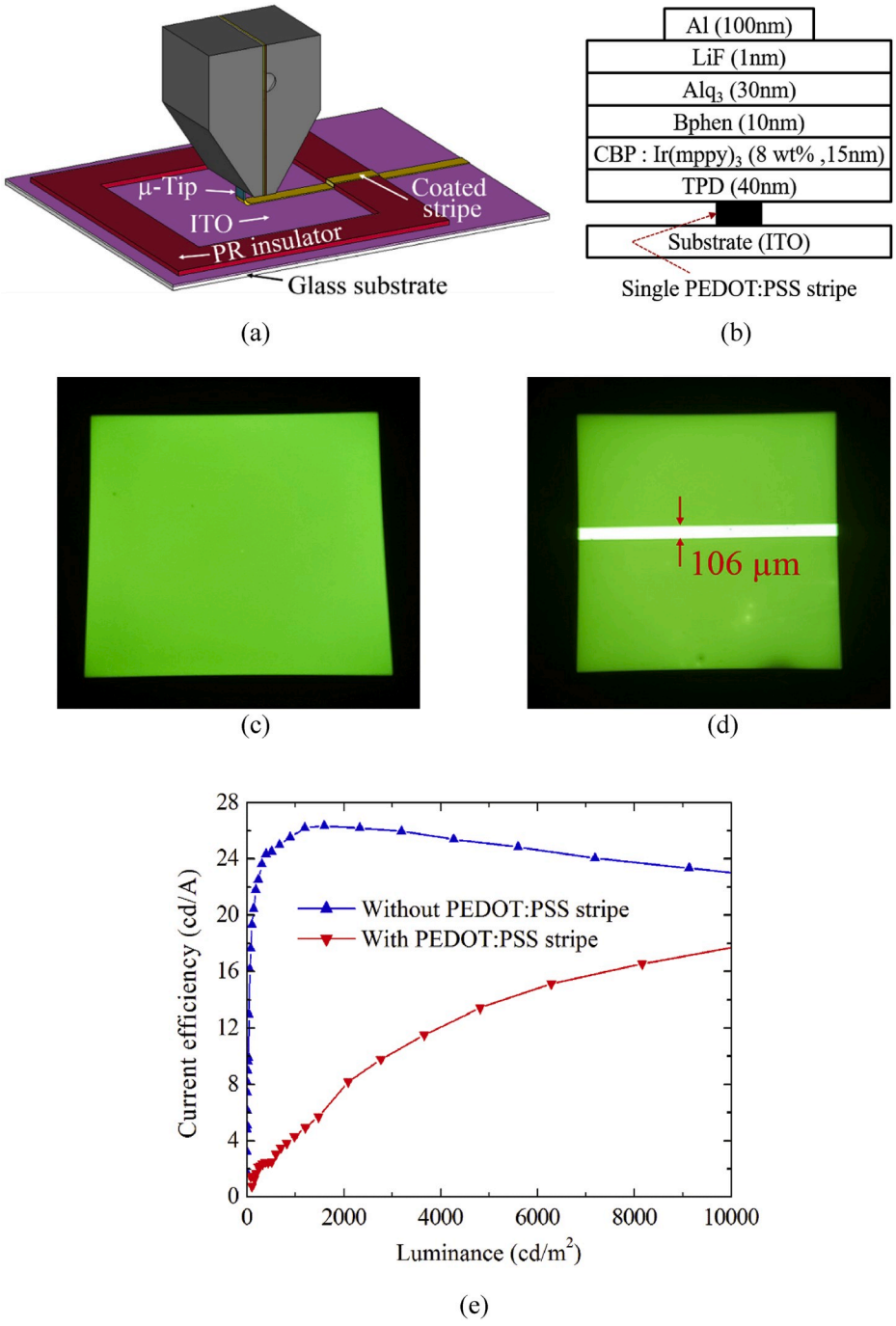

Fig. 7. (a) Schematic view of single stripe coating on ITO substrate with a PR insulator, (b) layer structure of green OLED device, images of light emission from 2 mm × 2 mm OLED devices at 8 V (c) without and (d) with a single PEDOT:PSS stripe coated using the LT-TIP, and (e) measured current efficiency as a function of luminance. (For interpretation of the references to colour in this figure legend, the reader is referred to the Web version of this article.)

degradation in the current efficiency of OLED with the PEDOT:PSS stripe (Fig. 7(e)). The width of the strong light-emitting stripe is about 106 μm, which is very close to that (98 μm) coated on the PET film roll at 20 mm/s. It is noted that stripe coating using the slot-die head with LT-TIP is not affected by the presence of 1.5-μm-thick PR insulating layer. Namely, any stripe broadening or thickening is not observed near the PR bank (at the perimeter of the emission area), a feature highly demanded for stripe coating of pixels with a PR bank.

To demonstrate the positive effect of the linearly tapered μ-tip in multiple stripe coating, we have fabricated 175 stripes using the meniscus guide with 175 LT-TIPs (Fig. 8). For comparison, we have also fabricated them using RW-TIPs. For multiple stripe coating, the flow rate was increased to 0.14 ml/min (175 × 0.8 μl/min). The success of multiple stripe coating depends sensitively on the μ-tip length. At the beginning of slot coating, the fluids from the neighboring outlets (slit channels) would merge together on the head lip and flow down the μ-tips without separation. To separate them and obtain fine stripes, we have increased the coating speed until right before line breakup occurs. If μ-tip is long, however, line breakup occurs at some μ-tips before the merged fluids are completely separated. To resolve it, we have reduced the μ-tip length from 250 μm to 100 μm. Since the R_T value is reduced accordingly, stable slot coating is expected. It is worth noting that such fluid merging may be avoidable by changing the surface of the head lip from hydrophilic to hydrophobic. It would suppress the lateral capillary flow and thus enable us to deploy the μ-tips closer (i.e., reduce the spacing between lines). In the presence of 175 μ-tips, the further slit channels (μ-tips) are away from the inlet located in the middle of the slot-die head (Fig. 1(a)), the less solution may flow through them. To tackle it, we have reduced the shim plate thickness from 50 μm to 25 μm, thereby ensuring the uniform pressure distribution inside the cavity (ink distribution chamber). Presented in Fig. 9(a) is the image of 175 stripes coated using LT-TIPs. The stripes are shown to be well defined. We have measured the stripe profiles and presented the results in Fig. 9 (b)–(c). As summarized in Table 2, the maximum coating speed (44 mm/s) with LT-TIPs is higher than that (29 mm/s) with RW-TIPs, a consequence expected from single stripe coating. The average width of stripes coated with RW-TIPs is observed to be 90 μm, which is much narrower than the μ-tip width (120 μm). It is because at the maximum coating speed, the w_n value becomes smaller than the μ-tip width at many RW-TIPs, which causes a fluctuation in the stripe width and thickness. If we reduce the coating speed to avoid it, the fluids from the neighboring outlets are merged. Unlike it, the average width of stripes coated with LT-TIPs is as narrow as 62 μm, which is slightly wider than the width (50 μm) of the μ-tip end. To quantify the film quality, we have also measured the inter-stripe width and thickness non-uniformity, defined as (maximum width (thickness) – minimum width (thickness))/average width (thickness). As

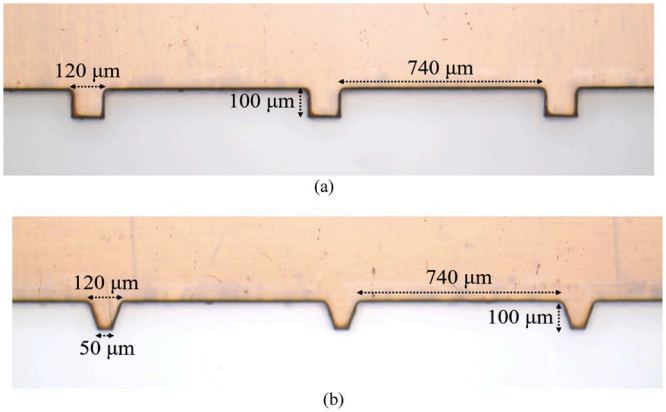

Fig. 8. Optical image of a meniscus guide with (a) 100-μm-long and 120-μm-wide RW-TIPs and (b) LT-TIPs for coating of multiple PEDOT:PSS stripes (175 lines).

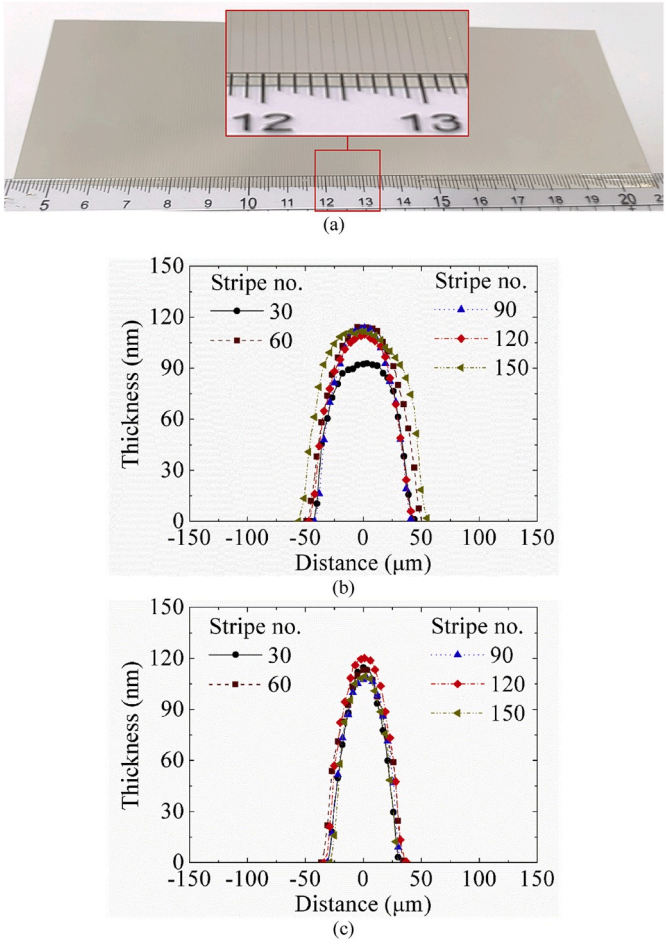

Fig. 9. (a) Image of 175 stripes coated using LT-TIPs and measured profiles of stripes coated with (b) RW-TIPs at 29 mm/s and (c) LT-TIPs at 44 mm/s.

Table 2
Measured width, thickness, and uniformity of 175 PEDOT:PSS stripes.

	RW-TIPs	LT-TIPs
Max. coating speed (mm/s)	29	44
Average stripe width (μm)	90	62
Average stripe thickness (nm)	106	113
Inter-stripe width non-uniformity (%)	31.1	20.9
Inter-stripe thickness non-uniformity (%)	25.4	16.8
Average spacing between stripes (μm)	775	802
Inter-stripe spacing non-uniformity (%)	8.9	1.4

expected, the inter-stripe width and thickness uniformities using LT-TIPs are superior to those using RW-TIPs. Similarly, we have measured the average spacing between stripes and the inter-stripe spacing non-uniformity. The average line spacing using LT-TIPs is measured to be 802 μm (the μ-tip spacing (740 μm in Fig. 8) + the average stripe width (62 μm)). If the stripe width is larger than the μ-tip width in the presence of RW-TIPs, the line spacing should be smaller than the μ-tip spacing (740 μm in Fig. 8). However, the average line spacing is measured to be 775 μm because the w_n value becomes smaller than the μ-tip width at many RW-TIPs (i.e., the solution is not distributed over the entire μ-tip end). As a result, the inter-stripe spacing uniformity is degraded with RW-TIPs, as evident in Fig. 10. Such a phenomenon disappears with LT-TIPs, leading to an increase in the inter-stripe spacing uniformity (98.6%), a feature highly desirable for coating of pixel array.

Finally, we have fabricated high-density PEDOT:PSS stripes using the slot-die head with two meniscus guides embedded (Fig. 1). Each

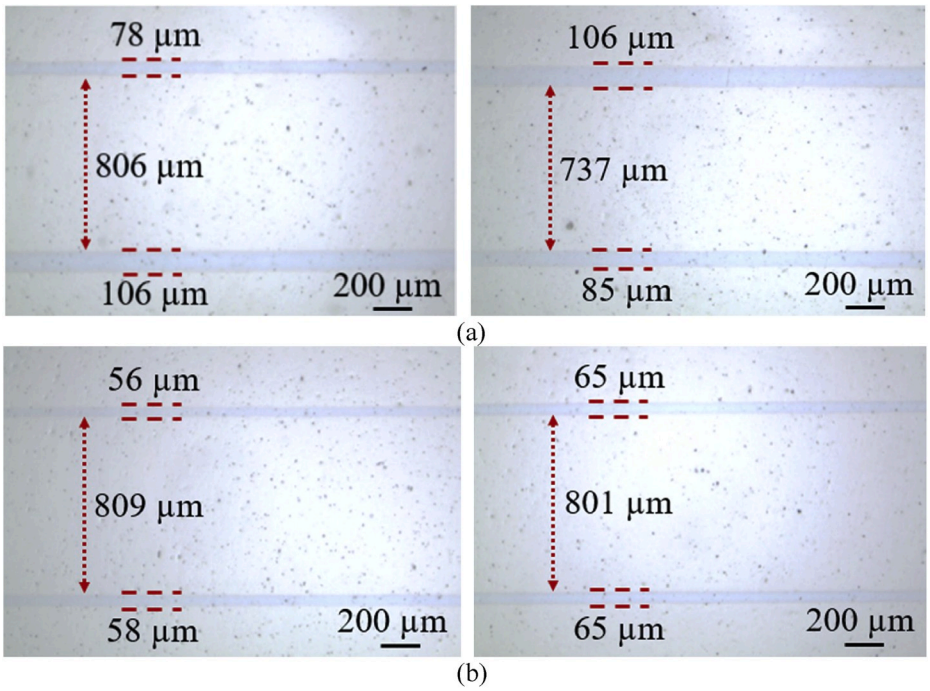

Fig. 10. Optical images of multiple PEDOT:PSS stripes (175 lines) coated with (a) RW-TIPs at the maximum coating speed of 29 mm/s and (b) LT-TIPs at 44 mm/s and measured at two different positions.

meniscus guide has 175 LT-TIPs. As evident in Fig. 11, we have successfully fabricated 350 stripes (59 SPI) at 44 mm/s. However, the uniformity in spacing between stripes is degraded to some extent. It is due to the fact that some misalignment between two meniscus guides occurs when embedding them manually into the slot-die head. It would be enhanced using an assembly (alignment) key, which can be installed in the slot-die head. We have also fabricated phosphorescent red OLED stripes atop the conductive PEDOT:PSS stripes. Since those PEDOT:PSS stripes are for an anode, we deposited 15-nm-thick KHI-001 (Duksan Neolux) for a HIL (Fig. 12(a)). In the EML, Bis[2-(3,5-dimethylphenyl)-4-methyl-quinoline](acetylacetonate)iridium(III) (Ir(mphmq)2(acac)) was doped (8 wt%) for red emission. Before loading the PET film with 350 PEDOT:PSS stripes into the vacuum chamber, we have cut 50 PEDOT:PSS stripes off because of its limited chamber size. Presented in Fig. 12(b) is the image of light emission from 300 red OLED stripes captured by an optical microscope and camera. For simplicity, no encapsulation was applied to the flexible OLED device. We have achieved red light emission from most of OLED stripes with the luminance of 350 cd/m^2 at 5V. Oxidization-induced partial light emission is observed from some OLED stripes. It may also occur if the PEDOT:PSS stripe is locally narrow and thin. Even so, the emission area (boundary) is shown to be well defined, demonstrating the potential applicability of R2R stripe coatings using such a slot-die head with linearly tapered μ-tips in large-area OLED displays. Using such a slot-die head, we can also fabricate non-aqueous organic thin-film stripes. However, the stripe profile may vary depending sensitively on the solvent properties (e.g., surface tension, viscosity, boiling point, and wettability (contact angle) on a substrate). In particular, the higher the wettability of the solution, the wider and thinner the stripes. Although the coating of PEDOT:PSS stripes was conducted within the area (width) of 150 mm, it can be extended further without line breakup using a slot-die head with a large width. However, much care is taken in designing the cavity structure (narrow rectangular or tilted cavity) to ensure the uniform pressure distribution across the slit channels.

4. Conclusion

We demonstrated that the linearly tapered μ-tip reduced the hydraulic resistance in the slit channel and narrowed the fluid stream near the μ-tip end, thereby providing the narrowest single PEDOT:PSS stripe at a relatively higher coating speed. Using the linearly tapered μ-tip with a width of 120 μm–50 μm and a length of 250 μm, we achieved a single PEDOT:PSS stripe as narrow as 98 μm and as thin as 89 nm at the maximum coating speed of 20 mm/s. For multiple stripe coating, the linearly tapered μ-tip also improved the inter-stripe width, thickness, and spacing uniformities. Using the linearly tapered μ-tips with a length

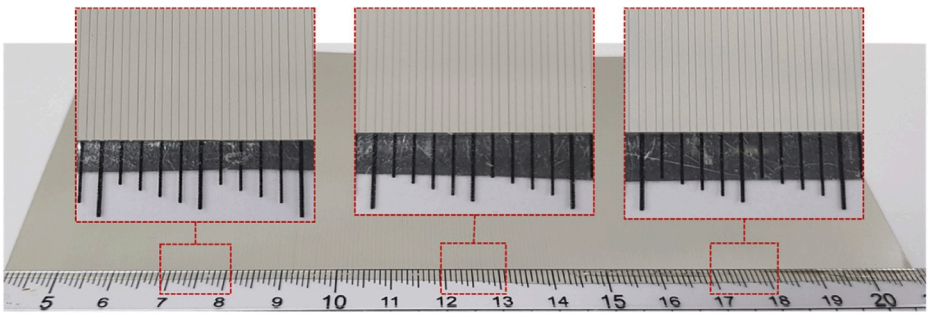

Fig. 11. Image of 350 stripes coated at 44 mm/s using the slot-die head with two meniscus guides embedded where LT-TIPs are formed.

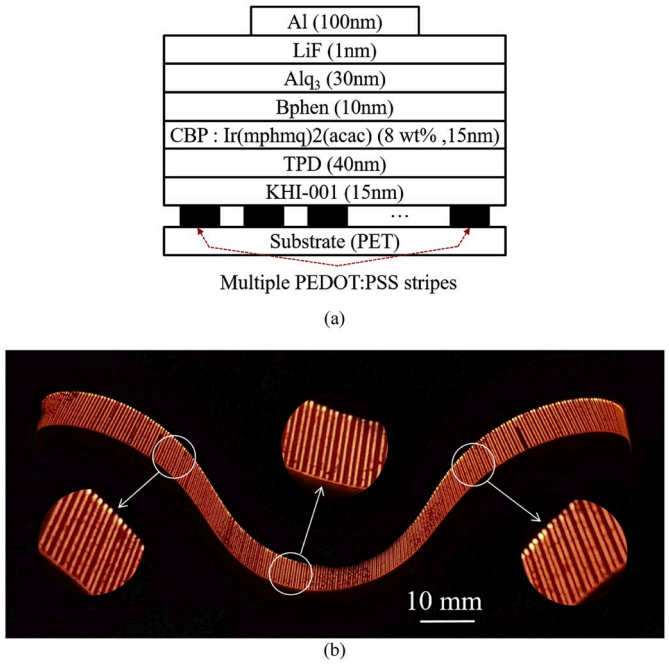

Fig. 12. (a) Layer structure of a red OLED device and (b) microscopic electroluminescent photos from curved 300 OLED stripes at 5 V (total length = 13 cm). (For interpretation of the references to colour in this figure legend, the reader is referred to the Web version of this article.)

of 100 μm, we fabricated 175 stripes with the average width of 62 μm and thickness of 113 nm at 44 mm/s. To fabricate high-density stripes, we employed the slot-die head with two meniscus guides (each has 175 linearly tapered μ-tips) embedded. Although the uniformity in spacing between stripes was degraded due to some misalignment between two meniscus guides, we successfully fabricated 350 PEDOT:PSS and 300 OLED stripes (59 stripes per inch) and achieved light emission from most of them with the luminance of 350 cd/m^2 at 5 V. The stripe density can be increased further by embedding more meniscus guides into a slot-die head with two middle dies or using two separate slot-die heads (each has two meniscus guides) without an overlap in the position of μ-tips.

Declaration of competing interest

The authors declare that they have no known competing financial interests or personal relationships that could have appeared to influence the work reported in this paper.

Acknowledgement

This research was supported by Basic Science Research Program through the National Research Foundation of Korea (NRF) (NRF-2018R1D1A1B07042248) funded by the Ministry of Education.

References

[1] R. Chesterfield, A. Johnson, C. Lang, M. Stainer, J. Ziebarth, Inf. Disp. 27 (2011) 24.
[2] S. Harkema, S. Mennema, M. Barink, H. Rooms, J.S. Wilson, T.V. Mol, D. Bollen, Proc. SPIE 7415 (2009), 74150T.
[3] J. Park, J. Lee, D. Shin, S. Park, J. Disp. Technol. 5 (2009) 306.
[4] Y.-M. Choi, K.-Y. Kim, E. Lee, J. Jo, T.-M. Lee, J. Infect. Dis. 16 (2015) 37.
[5] D.-Y. Shin, Y. Lee, C.H. Kim, Thin Solid Films 517 (2009) 6112.
[6] N. Lu, D.-H. Kim, Soft Robot. 1 (2014) 53.
[7] H. Liu, W. Xu, W. Tan, X. Zhu, J. Wang, J. Peng, Y. Cao, J. Colloid Interface Sci. 465 (2016) 106.
[8] M. Singh, H.M. Haverinen, P. Dhagat, G.E. Jabbour, Adv. Mater. 22 (2010) 673.
[9] D. Soltman, V. Subramanian, Langmuir 24 (2008) 2224.
[10] D. Deganello, Printing techniques for the fabrication of OLEDs, in: A. Buckley (Ed.), Organic Light-Emitting Diodes (OLEDs): Materials, Devices and Applications, Woodhead Publishing Limited, Cambridge, UK, 2013, p. 360.
[11] F.C. Krebs, Sol. Energy Mater. Sol. Cells 93 (2009) 394.
[12] R.R. Søndergaard, M. Hösel, F.C. Krebs, J. Polym. Sci. B Polym. Phys. 51 (2013) 16.
[13] M.S. Carvalho, H.S. Kheshgi, AlChE J 46 (2000) 1907.
[14] C.F. Lin, D.S. Wong, T. Liu, P. Wu, Adv. Polym. Technol. 29 (2010) 31.
[15] B. Park, O.E. Kwon, S.H. Yun, H.G. Jeon, Y.H. Huh, J. Mater. Chem. C 2 (2014) 8614.
[16] T.T. Larsen-Olsen, B. Andreasen, T.R. Andersen, A.P.L. Böttiger, E. Bundgaard, K. Norrman, J.W. Andreasen, M. Jørgensen, F.C. Krebs, Sol. Energy Mater. Sol. Cells 97 (2012) 22.
[17] A. Sandström, H.F. Dam, F.C. Krebs, L. Edman, Nat. Commun. 3 (2012) 1002.
[18] S.-H. Wen, T.-J. Liu, Polym. Eng. Sci. 35 (1995) 759.
[19] G.H. Han, S.H. Lee, W.-G. Ahn, J. Nam, H.W. Jung, J. Coating Technol. Res. 11 (2014) 19.
[20] G.-E. Kim, D.-K. Shin, J.-Y. Lee, J.W. Park, Org. Electron. 66 (2019) 116.
[21] K.W. Oh, K. Lee, B. Ahn, E.P. Furlani, Lab Chip 12 (2012) 515.
[22] D.E. Angelescu, Highly Integrated Microfluidics Design, Artech House, 2011.
[23] N.A. Mortensen, F. Okkels, H. Bruus, Phys. Rev. E: Stat., Nonlinear, Soft Matter Phys. 71 (2005), 057301.